Edge states and topological invariants of non-Hermitian systems

Shunyu Yao[1] and Zhong Wang[1,2,*]

[1] Institute for Advanced Study, Tsinghua University, Beijing, 100084, China
[2] Collaborative Innovation Center of Quantum Matter, Beijing, 100871, China

The bulk-boundary correspondence is among the central issues of non-Hermitian topological states. We show that a previously overlooked "non-Hermitian skin effect" necessitates redefinition of topological invariants in a generalized Brillouin zone. The resultant phase diagrams dramatically differ from the usual Bloch theory. Specifically, we obtain the phase diagram of non-Hermitian Su-Schrieffer-Heeger model, whose topological zero modes are determined by the non-Bloch winding number instead of the Bloch-Hamiltonian-based topological number. Our work settles the issue of the breakdown of conventional bulk-boundary correspondence and introduces the non-Bloch bulk-boundary correspondence.

Introduction.–Topological materials are characterized by robust boundary states immune to perturbations[1–5]. According to the principle of bulk-boundary correspondence, the existence of boundary states is dictated by the bulk topological invariants, which, in the band-theory framework, are defined in terms of the Bloch Hamiltonian. The Hamiltonian is often assumed to be Hermitian. In many physical systems, however, non-Hermitian Hamiltonians are more appropriate[6, 7]. For example, they are widely used in describing open systems[8–17], wave systems with gain and loss[18–40] (e.g. photonic and acoustic [41–44]), and solid-state systems where electron-electron interactions or disorders introduce a non-Hermitian self energy into the effective Hamiltonian of quasiparticle[45–47]. With these physical motivations, there have recently been growing efforts, both theoretically[48–78] and experimentally[79–85], to investigate topological phenomena of non-Hermitian Hamiltonians.

Among the key issues is the fate of bulk-boundary correspondence in non-Hermitian systems. Recently, numerical results in a one-dimensional (1D) model show that open-boundary spectra look notably different from periodic-boundary ones, which seems to indicate a complete breakdown of bulk-boundary correspondence[49, 86]. In view of this breakdown, a possible scenario is that the topological edge states depend on all sample details, without any general rule telling their existence or absence. Here, we ask the following questions: Is there a generalized bulk-boundary correspondence? Are there bulk topological invariants responsible for the topological edge states? Affirmative answers are obtained in this paper.

We start from solving a 1D model. Interestingly, all the eigenstates of an open chain are found to be localized near the boundary (dubbed "non-Hermtian skin effect"), in contrast to the extended Bloch waves in Hermitian cases. In the simplest situations, this effect can be understood in terms of an imaginary gauge field[87, 88]. We show that the non-Hermitian skin effect has dramatic consequences in establishing a "non-Bloch bulk-boundary correspondence" in which the topological boundary modes are determined by "non-Bloch topological invariants".

Previous non-Hermitian topological invariants[48–56] are formulated in terms of the Bloch Hamiltonian. The crucial non-Bloch-wave nature of eigenstates (non-Hermitian skin effect) is untouched, therefore, the number of topological edge modes is not generally related to these topological invariants. In view of the non-Hermitian skin effect, we introduce a non-Bloch topological invariant, which faithfully determines the number of topological edge modes. It embodies the non-Bloch bulk-boundary correspondence of non-Hermitian systems.

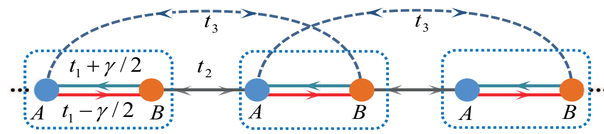

FIG. 1. Non-Hermitian SSH model. The dotted box indicates the unit cell.

Model.–The non-Hermitian Su-Schrieffer-Heeger (SSH) model[89][90] is pictorially shown in Fig.1. Related models are relevant to quite a few experiments[79, 82, 91]. The Bloch Hamiltonian is

$$H(k) = d_x\sigma_x + (d_y + i\frac{\gamma}{2})\sigma_y, \tag{1}$$

where $d_x = t_1 + (t_2 + t_3)\cos k$, $d_y = (t_2 - t_3)\sin k$, and $\sigma_{x,y}$ are the Pauli matrices. A mathematically equivalent model was studied in Ref. [49], where σ_y was replaced by σ_z; as such, the physical interpretation was not SSH. The model has a chiral symmetry[3] $\sigma_z^{-1}H(k)\sigma_z = -H(k)$, which ensures that the eigenvalues appear in $(E, -E)$ pairs: $E_\pm(k) = \pm\sqrt{d_x^2 + (d_y + i\gamma/2)^2}$. Let us first take $t_3 = 0$ for simplicity (nonzero t_3 will be included later). The energy gap closes at the exceptional points $(d_x, d_y) = (\pm\gamma/2, 0)$, which requires $t_1 = t_2 \pm \gamma/2$ $(k = \pi)$ or $t_1 = -t_2 \pm \gamma/2$ $(k = 0)$.

The open-boundary spectrum is noticeably different from that of periodic boundary[49][92], which can be seen in the numerical spectra of real-space Hamiltonian of an open chain [Fig.2]. The zero modes are robust to perturbation [Fig.2(d)], which indicates their topological origin. A transition point is located at $t_1 \approx 1.20$, which is a quite unremarkable point from the perspective of $H(k)$ whose spectrum is gapped there ($|E_\pm(k)| \neq 0$). As such, the topology of $H(k)$ cannot determine the zero modes, which challenges the familiar Hermitian wis-

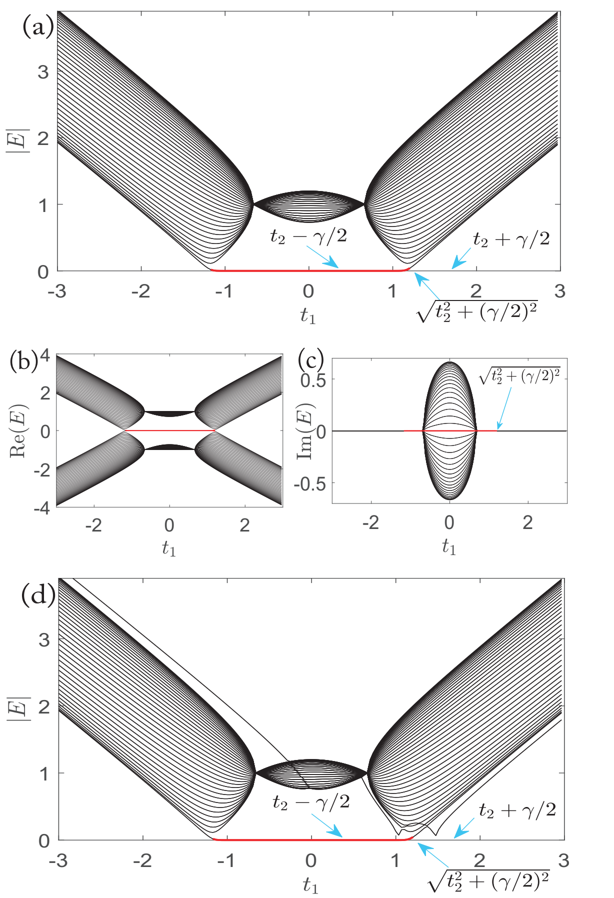

FIG. 2. Numerical spectra of of an open chain with length $L = 40$ (unit cell). $t_2 = 1$, $\gamma = 4/3$; t_1 varies in $[-3, 3]$. (a) $|E|$ as functions of t_1. The zero-mode line is shown in red (twofold degenerate, ignoring an indiscernible split). The true transition point ($\sqrt{t_2^2+(\gamma/2)^2} \approx 1.20$) and the $H(k)$-gap-closing points ($t_2 \pm \gamma/2$) are indicated by arrows. (b,c) The real and imaginary parts of E. (d) The same as (a) except that the value of t_1 at the leftmost bond is replaced by $t_1 - 0.8$, which generates additional nonzero modes, but the zero modes are unaffected.

dom. The question arises: What topological invariant predicts the zero modes?

Shortcut solution.–To gain insights, we analytically solve an open chain. The wavefunction is written as $|\psi\rangle = (\psi_{1,A}, \psi_{1,B}, \psi_{2,A}, \psi_{2,B}, \cdots, \psi_{L,A}, \psi_{L,B})^T$. We first present a shortcut, which is applicable only to the $t_3 = 0$ case. The real-space eigen-equation $H|\psi\rangle = E|\psi\rangle$ is equivalent to $\bar{H}|\bar{\psi}\rangle = E|\bar{\psi}\rangle$ with $|\bar{\psi}\rangle = S^{-1}|\psi\rangle$ and

$$\bar{H} = S^{-1}HS. \tag{2}$$

We can judiciously choose S in this similarity transformation. Let us take S to be a diagonal matrix whose diagonal elements are $\{1, r, r, r^2, r^2, \cdots, r^{L-1}, r^{L-1}, r^L\}$, then in $\bar{H}$ we have $r^{\pm1}(t_1 \pm \gamma/2)$ in the place of $t_1 \pm \gamma/2$ (Fig.1). If we take $r = \sqrt{|\frac{t_1-\gamma/2}{t_1+\gamma/2}|}$, $\bar{H}$ becomes the standard SSH model for $|t_1| > |\gamma/2|$, with intracell and intercell hoppings

$$\bar{t}_1 = \sqrt{(t_1-\gamma/2)(t_1+\gamma/2)}, \quad \bar{t}_2 = t_2. \tag{3}$$

The k-space expression is

$$\bar{H}(k) = (\bar{t}_1 + \bar{t}_2 \cos k)\sigma_x + \bar{t}_2 \sin k \sigma_y. \tag{4}$$

The transition points are $\bar{t}_1 = \bar{t}_2$, namely

$$t_1 = \pm\sqrt{t_2^2 + (\gamma/2)^2}. \tag{5}$$

For the parameters in Fig.2, Eq.(5) gives $t_1 \approx \pm1.20$. Note that any $H(k)$-based topological invariants[48–56] can jump only at $t_1 = \pm t_2 \pm \gamma/2$, where the gap of $H(k)$ closes.

A bulk eigenstate $|\bar{\psi}_l\rangle$ of Hermitian $\bar{H}$ is extended, therefore, H's eigenstate $|\psi_l\rangle = S|\bar{\psi}_l\rangle$ is exponentially localized at an end of the chain when $\gamma \neq 0$. It implies that the usual Bloch phase factor e^{ik} is replaced by $\beta \equiv re^{ik}$ in the open-boundary system (i.e., the wavevector acquires an imaginary part: $k \to k - i\ln r$). Although this intuitive picture is based on the shortcut solution, we believe that the exponential-decay behavior of eigenstates ("non-Hermitian skin effect") is a general feature of non-Hermitian bands.

Generalizable solution.–The intuitive shortcut solution has limitations; e.g., it is inapplicable when $t_3 \neq 0$. Here, we re-derive the solution in a more generalizable way (still focusing on $t_3 = 0$ for simplicity). The real-space eigen-equation leads to $t_2\psi_{n-1,B} + (t_1 + \frac{\gamma}{2})\psi_{n,B} = E\psi_{n,A}$ and $(t_1 - \frac{\gamma}{2})\psi_{n,A} + t_2\psi_{n+1,A} = E\psi_{n,B}$ in the bulk of chain. We take the ansatz that $|\psi\rangle = \sum_j |\phi^{(j)}\rangle$, where each $|\phi^{(j)}\rangle$ takes the exponential form (omitting the j index temporarily): $(\phi_{n,A}, \phi_{n,B}) = \beta^n(\phi_A, \phi_B)$, which satisfies

$$[(t_1 + \frac{\gamma}{2}) + t_2\beta^{-1}]\phi_B = E\phi_A, \ \ [(t_1 - \frac{\gamma}{2}) + t_2\beta]\phi_A = E\phi_B. \tag{6}$$

Therefore, we have

$$[(t_1 - \frac{\gamma}{2}) + t_2\beta][(t_1 + \frac{\gamma}{2}) + t_2\beta^{-1}] = E^2, \tag{7}$$

which has two solutions, namely $\beta_{1,2}(E) = \frac{E^2+\gamma^2/4-t_1^2-t_2^2 \pm \sqrt{(E^2+\gamma^2/4-t_1^2-t_2^2)^2-4t_2^2(t_1^2-\gamma^2/4)}}{2t_2(t_1+\gamma/2)}$, where $+(-)$ corresponds to $\beta_1(\beta_2)$. In the $E \to 0$ limit, we have

$$\beta_{1,2}^{E\to0} = -\frac{t_1-\gamma/2}{t_2}, \ -\frac{t_2}{t_1+\gamma/2}. \tag{8}$$

They can also be seen from Eq.(6). These two solutions correspond to $\phi_B = 0$ and $\phi_A = 0$, respectively.

Restoring the j index in $|\phi^{(j)}\rangle$, we have

$$\phi_A^{(j)} = \frac{E}{t_1 - \gamma/2 + t_2\beta_j}\phi_B^{(j)}, \quad \phi_B^{(j)} = \frac{E}{t_1 + \gamma/2 + t_2\beta_j^{-1}}\phi_A^{(j)}. \tag{9}$$

These two equations are equivalent because of Eq.(7). The general solution is written as a linear combination:

$$\begin{pmatrix}\psi_{n,A}\\ \psi_{n,B}\end{pmatrix} = \beta_1^n\begin{pmatrix}\phi_A^{(1)}\\ \phi_B^{(1)}\end{pmatrix} + \beta_2^n\begin{pmatrix}\phi_A^{(2)}\\ \phi_B^{(2)}\end{pmatrix}, \tag{10}$$

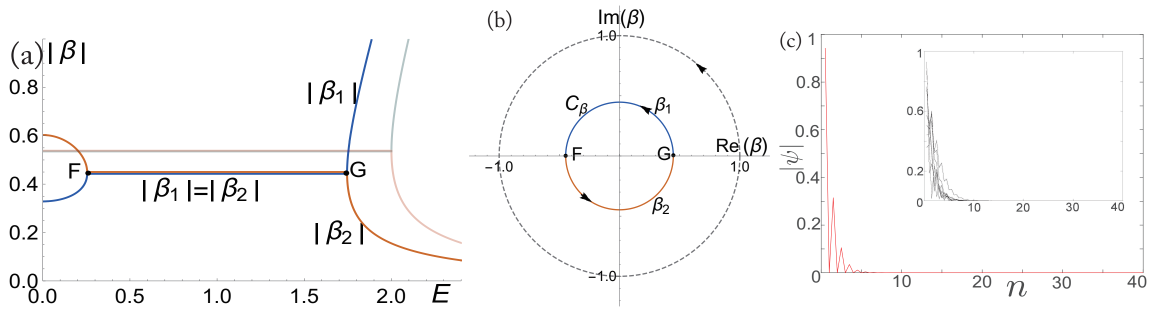

FIG. 3. (a) $|\beta_j|$-E curves from Eq.(7). $t_1 = 1$ (dark color) and $\sqrt{t_2^2 + (\gamma/2)^2} \approx 1.20$ (light color). (b) Complex-valued β_j's form a closed loop C_β, which is a circle for the present model [by Eq.(13)]. The shown one is for $t_1 = 1$. C_β can be viewed as a deformed Brillouin zone that generalizes the usual one. In Hermitian cases, C_β is a unit circle (dashed line). (c) Profile of a zero mode (main figure) and eight randomly chosen bulk eigenstates (inset), illustrating the "non-Hermitian skin effect" found in the analytic solution, namely, all the bulk eigenstates are localized near the boundary. $t_1 = 1$. Common parameters: $t_2 = 1, \gamma = 4/3$.

which should satisfy the boundary condition

$$(t_1 + \frac{\gamma}{2})\psi_{1,B} - E\psi_{1,A} = 0, \ \ (t_1 - \frac{\gamma}{2})\psi_{L,A} - E\psi_{L,B} = 0. \quad (11)$$

Together with Eq.(9), they lead to

$$\beta_1^{L+1}(t_1 - \gamma/2 + t_2\beta_2) = \beta_2^{L+1}(t_1 - \gamma/2 + t_2\beta_1). \quad (12)$$

We are concerned about the spectrum for a long chain, which necessitates $|\beta_1| = |\beta_2|$ for the bulk eigenstates. If not, suppose that $|\beta_1| < |\beta_2|$, we would be able to discard the tiny β_1^{L+1} term in Eq.(12), and the equation becomes $\beta_2 = 0$ or $t_1 - \gamma/2 + t_2\beta_1 = 0$ (without the appearance of L). As a bulk-band property, $|\beta_1(E)| = |\beta_2(E)|$ remains valid in the presence of perturbations near the edges [e.g., Fig.2(d)], and essentially determines the bulk-band energies[93]. Combined with $\beta_1\beta_2 = \frac{t_1-\gamma/2}{t_1+\gamma/2}$ coming from Eq.(7), $|\beta_1| = |\beta_2|$ leads to

$$|\beta_j| = r \equiv \sqrt{\left|\frac{t_1 - \gamma/2}{t_1 + \gamma/2}\right|} \quad (13)$$

for bulk eigenstates (i.e., eigenstates in the continuum spectrum). The same r has just been used in the shortcut solution.

We emphasize that $r < 1$ indicates that all the eigenstates are localized at the left end of the chain [see Fig.3(c) for illustration][94][95]. In Hermitian systems, the orthogonality of eigenstates excludes this "non-Hermitian skin effect".

There are various ways to re-derive the transition points in Eq.(5). To introduce one of them, we first plot in Fig.3(a) the $|\beta|$-E curve solved from Eq.(7) for $t_1 = t_2 = 1, \gamma = 4/3$. The spectrum is real for this set of parameters, therefore, no imaginary part of E is needed (This reality is related to PT symmetry[6, 7]). The expected $|\beta_1| = |\beta_2| = r$ relation is found on the line FG (Fig.3(a)), which is associated with bulk spectra. As t_1 is increased from 1, F moves towards left, and finally hits the $|\beta|$ axis ($E = 0$ axis). Apparently, it occurs when $|\beta_1^{E\to 0}| = |\beta_2^{E\to 0}| = r$. Inserting Eq.(8) into this equation, we have

$$t_1 = \pm\sqrt{t_2^2 + (\gamma/2)^2} \quad \text{or} \quad \pm\sqrt{-t_2^2 + (\gamma/2)^2}. \quad (14)$$

At these points, the open-boundary continuum spectra touch zero energy, enabling topological transitions.

A simpler way to re-derive Eq.(5) is to calculate the open-boundary spectra. According to Eq.(13), we can take $\beta = re^{ik}$ ($k \in [0, 2\pi]$) in Eq.(7) to obtain the spectra:

$$\begin{aligned} E^2(k) =& t_1^2 + t_2^2 - \gamma^2/4 + t_2\sqrt{|t_1^2 - \gamma^2/4|}[\text{sgn}(t_1 + \gamma/2)e^{ik} \\ &+ \text{sgn}(t_1 - \gamma/2)e^{-ik}], \end{aligned} \quad (15)$$

which recovers the spectrum of SSH model when $\gamma = 0$. The spectra are real when $|t_1| > |\gamma|/2$. Eq.(14) can be readily re-derived as the gap-closing condition of Eq.(15) ($|E(k)| = 0$).

Before proceeding, we comment on a subtle issue in the standard method of finding zero modes. For concreteness, let us consider the present model, and focus on zero modes at the left end of a long chain. One can see that $|\psi^{\text{zero}}\rangle$ with $(\psi_{n,A}^{\text{zero}}, \psi_{n,B}^{\text{zero}}) = (\beta_1^{E\to 0})^n(1, 0)$ appears as a zero-energy eigenstate (see Eq.(8) for $\beta_1^{E\to 0}$). In the standard approach, the normalizable condition $|\beta_1^{E\to 0}| < 1$ is imposed, and the transition points satisfy $|\beta_1^{E\to 0}| = 1$, which predicts $t_1 = t_2 + \gamma/2$ as a transition point, being consistent with the gap closing of $H(k)$. Such an apparent but misleading consistency has hidden the true transition points and topological invariants in quite a few previous studies of non-Hermitian models. The implicit assumption was that the bulk eigenstates are extended Bloch waves with $|\beta| = 1$, into which the zero modes merge at transitions. In reality, the bulk eigenstates have $|\beta| = r$ (eigenstate skin effect); therefore, the true merging-into-bulk condition is

$$|\beta_1^{E\to 0}| = r, \quad (16)$$

which correctly produces $t_1 = \sqrt{t_2^2 + (\gamma/2)^2}$. This is a manifestation of the non-Bloch bulk-boundary correspondence.

Non-Bloch topological invariant.–The bulk-boundary correspondence is fulfilled if we can find a bulk topological invariant that determines the edge modes. Previous constructions take $H(k)$ as the starting point[48–56], which should be revised in view of the non-Hermitian skin effect. The usual Bloch waves carry a pure phase factor e^{ik}, whose role is now

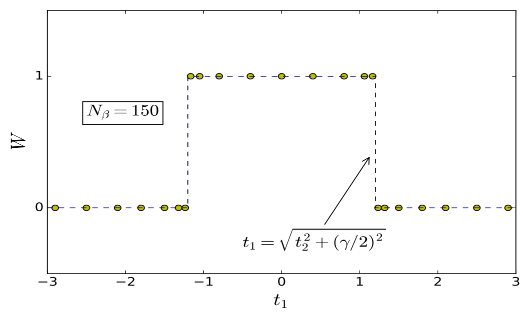

FIG. 4. Numerical result of topological invariant. N_β is the number of grid point on C_β. $t_2 = 1, \gamma = 4/3$.

played by β. In addition to the phase factor, β has a modulus $|\beta| \neq 1$ in general [e.g., Eq.(13)]. Therefore, we start from the "non-Bloch Hamiltonian" obtained from $H(k)$ by the replacement $e^{ik} \to \beta, e^{-ik} \to \beta^{-1}$:

$$H(\beta) = (t_1 - \frac{\gamma}{2} + \beta t_2)\sigma_- + (t_1 + \frac{\gamma}{2} + \beta^{-1} t_2)\sigma_+, \tag{17}$$

where $\sigma_\pm = (\sigma_x \pm i\sigma_y)/2$. We have taken $t_3 = 0$ for simplicity. As explained in both the shortcut and generalizable solutions, β takes values in a non-unit circle $|\beta| = r$ (In other words, k acquires an imaginary part $-i \ln r$). It is notable that the open-boundary spectra in Eq.(15) are given by $H(\beta)$ instead of $H(k)$. The right and left eigenvectors are defined by

$$H(\beta)|u_\mathrm{R}\rangle = E(\beta)|u_\mathrm{R}\rangle, \quad H^\dagger(\beta)|u_\mathrm{L}\rangle = E^*(\beta)|u_\mathrm{L}\rangle. \tag{18}$$

Chiral symmetry ensures that $|\tilde{u}_\mathrm{R}\rangle \equiv \sigma_z|u_\mathrm{R}\rangle$ and $|\tilde{u}_\mathrm{L}\rangle \equiv \sigma_z|u_\mathrm{L}\rangle$ is also right and left eigenvector, with eigenvalues $-E$ and $-E^*$, respectively. In fact, one can diagonalize the matrix as $H(\beta) = TJT^{-1}$ with $J = \begin{pmatrix} E & \\ & -E \end{pmatrix}$, then each column of T and $(T^{-1})^\dagger$ is a right and left eigenvector, respectively, and the normalization condition $\langle u_\mathrm{L}|u_\mathrm{R}\rangle = \langle \tilde{u}_\mathrm{L}|\tilde{u}_\mathrm{R}\rangle = 1, \langle u_\mathrm{L}|\tilde{u}_\mathrm{R}\rangle = \langle \tilde{u}_\mathrm{L}|u_\mathrm{R}\rangle = 0$ is guaranteed. As a generalization of the usual "Q matrix"[3], we define

$$Q(\beta) = |\tilde{u}_\mathrm{R}(\beta)\rangle\langle\tilde{u}_\mathrm{L}(\beta)| - |u_\mathrm{R}(\beta)\rangle\langle u_\mathrm{L}(\beta)|, \tag{19}$$

which is off-diagonal due to the chiral symmetry $\sigma_z^{-1} Q \sigma_z = -Q$, namely $Q = \begin{pmatrix} & q \\ q^{-1} & \end{pmatrix}$. Now we introduce the non-Bloch winding number:

$$W = \frac{i}{2\pi} \int_{C_\beta} q^{-1} dq. \tag{20}$$

Crucially, it is defined on the "generalized Brillouin zone" C_β [Fig.3(b)]. It is useful to mention that the conventional formulations using $H(k)$ may sometimes produce correct phase diagrams, if C_β happens to be a unit circle[96].

The numerical results for $t_3 = 0$ is shown in Fig.4, which is consistent with the analytical spectra obtained above. Quantitatively, $2W$ counts the total number of robust zero modes at the left and right ends. For example, corresponding to Fig.2, there are two zero modes for $t_1 \in [-\sqrt{t_2^2 + (\gamma/2)^2}, \sqrt{t_2^2 + (\gamma/2)^2}]$, and none elsewhere. The analytic solution shows that, for $[t_2 - \gamma/2, \sqrt{t_2^2 + (\gamma/2)^2}]$, both modes live at the left end; for $[-t_2+\gamma/2, t_2-\gamma/2]$, one for each end; and for $[-\sqrt{t_2^2 + (\gamma/2)^2}, -t_2 + \gamma/2]$, both at the right end. Thus, the $H(k)$-gap closing points $\pm(t_2 - \gamma/2)$ are where zero modes migrate from one end to the other, conserving the total mode number. In fact, one can see $|\beta_{j=1\,\mathrm{or}\,2}^{E\to 0}| = 1$ at $\pm(t_2 - \gamma/2)$, indicating the penetration into bulk.

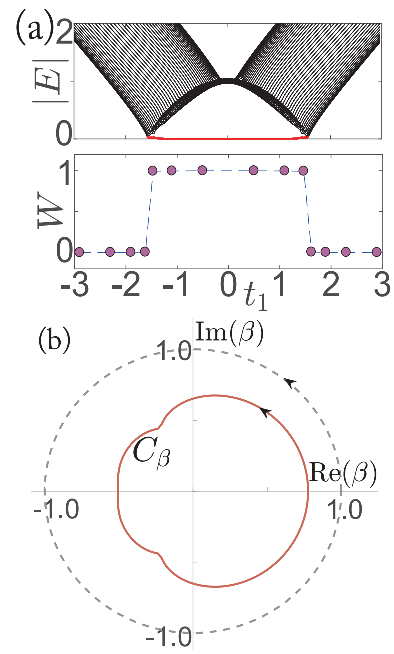

FIG. 5. The nonzero t_3 case. (a) Upper panel: Spectrum of an open chain; $t_2 = 1, \gamma = 4/3, t_3 = 1/5$; $L = 100$. Lower panel: topological invariant calculated using 200 grid points on C_β. The transition points are $t_1 \approx \pm 1.56$. (b) C_β for $t_1 = 1.1$.

To provide a more generic exemplification, we take a nonzero t_3. Now we find[93] that C_β is no longer a circle (bulk eigenstates with different energies have different $|\beta|$), yet $2W$ correctly predicts the total zero-mode number (Fig.5).

Finally, we remarked that Eq.(20) can be generalized to multi-band systems. Each pair of bands (labeled by l) possesses a $C_\beta^{(l)}$ curve, and the Q matrix [Eq.(19)] becomes $Q^{(l)}$, each one defining a winding number $W^{(l)}$ (with matrix trace). The topological invariant is $W = \sum_l W^{(l)}$.

Conclusions.–Through the analytic solution of non-Hermitian SSH model, we explained why the usual bulk-boundary correspondence breaks down, and how the non-Bloch bulk-boundary correspondence takes its place. Two of the key concepts are the non-Hermitian skin effect and generalized Brillouin zone. We formulate the generalized bulk-boundary correspondence by introducing a precise topological invariant that faithfully predicts the topological edge modes. The physics presented here can be generalized to a rich variety of non-Hermitian systems, which will be left for future studies.

Acknowledgements.–This work is supported by NSFC under Grant No. 11674189.

* wangzhongemail@gmail.com

[1] M. Z. Hasan and C. L. Kane, "*Colloquium* : Topological insulators," Rev. Mod. Phys. **82**, 3045–3067 (2010).

[2] Xiao-Liang Qi and Shou-Cheng Zhang, "Topological insulators and superconductors," Rev. Mod. Phys. **83**, 1057–1110 (2011).

[3] Ching-Kai Chiu, Jeffrey C. Y. Teo, Andreas P. Schnyder, and Shinsei Ryu, "Classification of topological quantum matter with symmetries," Rev. Mod. Phys. **88**, 035005 (2016).

[4] B Andrei Bernevig and Taylor L Hughes, *Topological insulators and topological superconductors* (Princeton University Press, Princeton, NJ, 2013).

[5] A. Bansil, Hsin Lin, and Tanmoy Das, "*Colloquium* : Topological band theory," Rev. Mod. Phys. **88**, 021004 (2016).

[6] Carl M Bender and Stefan Boettcher, "Real spectra in non-hermitian hamiltonians having p t symmetry," Physical Review Letters **80**, 5243 (1998).

[7] Carl M Bender, "Making sense of non-hermitian hamiltonians," Reports on Progress in Physics **70**, 947 (2007).

[8] Ingrid Rotter, "A non-hermitian hamilton operator and the physics of open quantum systems," Journal of Physics A: Mathematical and Theoretical **42**, 153001 (2009).

[9] Simon Malzard, Charles Poli, and Henning Schomerus, "Topologically protected defect states in open photonic systems with non-hermitian charge-conjugation and parity-time symmetry," Phys. Rev. Lett. **115**, 200402 (2015).

[10] H. J. Carmichael, "Quantum trajectory theory for cascaded open systems," Phys. Rev. Lett. **70**, 2273–2276 (1993).

[11] Bo Zhen, Chia Wei Hsu, Yuichi Igarashi, Ling Lu, Ido Kaminer, Adi Pick, Song-Liang Chua, John D Joannopoulos, and Marin Soljačić, "Spawning rings of exceptional points out of dirac cones," Nature **525**, 354 (2015).

[12] Sebastian Diehl, Enrique Rico, Mikhail A Baranov, and Peter Zoller, "Topology by dissipation in atomic quantum wires," Nature Physics **7**, 971–977 (2011).

[13] Hui Cao and Jan Wiersig, "Dielectric microcavities: Model systems for wave chaos and non-hermitian physics," Rev. Mod. Phys. **87**, 61–111 (2015).

[14] Youngwoon Choi, Sungsam Kang, Sooin Lim, Wookrae Kim, Jung-Ryul Kim, Jai-Hyung Lee, and Kyungwon An, "Quasieigenstate coalescence in an atom-cavity quantum composite," Phys. Rev. Lett. **104**, 153601 (2010).

[15] Pablo San-Jose, Jorge Cayao, Elsa Prada, and Ramón Aguado, "Majorana bound states from exceptional points in non-topological superconductors," Scientific reports **6**, 21427 (2016).

[16] Tony E. Lee and Ching-Kit Chan, "Heralded magnetism in non-hermitian atomic systems," Phys. Rev. X **4**, 041001 (2014).

[17] Tony E. Lee, Florentin Reiter, and Nimrod Moiseyev, "Entanglement and spin squeezing in non-hermitian phase transitions," Phys. Rev. Lett. **113**, 250401 (2014).

[18] K. G. Makris, R. El-Ganainy, D. N. Christodoulides, and Z. H. Musslimani, "Beam dynamics in $\mathcal{PT}$ symmetric optical lattices," Phys. Rev. Lett. **100**, 103904 (2008).

[19] S. Longhi, "Bloch oscillations in complex crystals with $\mathcal{PT}$ symmetry," Phys. Rev. Lett. **103**, 123601 (2009).

[20] Shachar Klaiman, Uwe Günther, and Nimrod Moiseyev, "Visualization of branch points in $\mathcal{PT}$-symmetric waveguides," Phys. Rev. Lett. **101**, 080402 (2008).

[21] Alois Regensburger, Christoph Bersch, Mohammad-Ali Miri, Georgy Onishchukov, Demetrios N Christodoulides, and Ulf Peschel, "Parity–time synthetic photonic lattices," Nature **488**, 167 (2012).

[22] S. Bittner, B. Dietz, U. Günther, H. L. Harney, M. Miski-Oglu, A. Richter, and F. Schäfer, "Pt-symmetry and spontaneous symmetry breaking in a microwave billiard," Phys. Rev. Lett. **108**, 024101 (2012).

[23] Christian E Rüter, Konstantinos G Makris, Ramy El-Ganainy, Demetrios N Christodoulides, Mordechai Segev, and Detlef Kip, "Observation of parity–time symmetry in optics," Nature physics **6**, 192 (2010).

[24] Zin Lin, Hamidreza Ramezani, Toni Eichelkraut, Tsampikos Kottos, Hui Cao, and Demetrios N. Christodoulides, "Unidirectional invisibility induced by $\mathcal{PT}$-symmetric periodic structures," Phys. Rev. Lett. **106**, 213901 (2011).

[25] Liang Feng, Ye-Long Xu, William S Fegadolli, Ming-Hui Lu, José EB Oliveira, Vilson R Almeida, Yan-Feng Chen, and Axel Scherer, "Experimental demonstration of a unidirectional reflectionless parity-time metamaterial at optical frequencies," Nature materials **12**, 108 (2013).

[26] A. Guo, G. J. Salamo, D. Duchesne, R. Morandotti, M. Volatier-Ravat, V. Aimez, G. A. Siviloglou, and D. N. Christodoulides, "Observation of $\mathcal{PT}$-symmetry breaking in complex optical potentials," Phys. Rev. Lett. **103**, 093902 (2009).

[27] M. Liertzer, Li Ge, A. Cerjan, A. D. Stone, H. E. Türeci, and S. Rotter, "Pump-induced exceptional points in lasers," Phys. Rev. Lett. **108**, 173901 (2012).

[28] B Peng, ŞK Özdemir, S Rotter, H Yilmaz, M Liertzer, F Monifi, CM Bender, F Nori, and L Yang, "Loss-induced suppression and revival of lasing," Science **346**, 328–332 (2014).

[29] Romain Fleury, Dimitrios Sounas, and Andrea Alù, "An invisible acoustic sensor based on parity-time symmetry," Nature communications **6**, 5905 (2015).

[30] Long Chang, Xiaoshun Jiang, Shiyue Hua, Chao Yang, Jianming Wen, Liang Jiang, Guanyu Li, Guanzhong Wang, and Min Xiao, "Parity–time symmetry and variable optical isolation in active–passive-coupled microresonators," Nature photonics **8**, 524 (2014).

[31] Hossein Hodaei, Absar U Hassan, Steffen Wittek, Hipolito Garcia-Gracia, Ramy El-Ganainy, Demetrios N Christodoulides, and Mercedeh Khajavikhan, "Enhanced sensitivity at higher-order exceptional points," Nature **548**, 187 (2017).

[32] Hossein Hodaei, Mohammad-Ali Miri, Matthias Heinrich, Demetrios N Christodoulides, and Mercedeh Khajavikhan, "Parity-time–symmetric microring lasers," Science **346**, 975–978 (2014).

[33] Liang Feng, Zi Jing Wong, Ren-Min Ma, Yuan Wang, and Xiang Zhang, "Single-mode laser by parity-time symmetry breaking," Science **346**, 972–975 (2014).

[34] Tiejun Gao, E Estrecho, KY Bliokh, TCH Liew, MD Fraser, Sebastian Brodbeck, Martin Kamp, Christian Schneider, Sven Höfling, Y Yamamoto, *et al.*, "Observation of non-hermitian degeneracies in a chaotic exciton-polariton billiard," Nature **526**, 554 (2015).

[35] Haitan Xu, David Mason, Luyao Jiang, and JGE Harris, "Topological energy transfer in an optomechanical system with exceptional points," Nature **537**, 80 (2016).

[36] Yuto Ashida, Shunsuke Furukawa, and Masahito Ueda, "Parity-time-symmetric quantum critical phenomena," Nature communications **8**, 15791 (2017).
[37] Kohei Kawabata, Yuto Ashida, and Masahito Ueda, "Information retrieval and criticality in parity-time-symmetric systems," Phys. Rev. Lett. **119**, 190401 (2017).
[38] Weijian Chen, Şahin Kaya Özdemir, Guangming Zhao, Jan Wiersig, and Lan Yang, "Exceptional points enhance sensing in an optical microcavity," Nature **548**, 192 (2017).
[39] Kun Ding, Guancong Ma, Meng Xiao, Z. Q. Zhang, and C. T. Chan, "Emergence, coalescence, and topological properties of multiple exceptional points and their experimental realization," Phys. Rev. X **6**, 021007 (2016).
[40] Charles A. Downing and Guillaume Weick, "Topological collective plasmons in bipartite chains of metallic nanoparticles," Phys. Rev. B **95**, 125426 (2017).
[41] T. Ozawa, H. M. Price, A. Amo, N. Goldman, M. Hafezi, L. Lu, M. Rechtsman, D. Schuster, J. Simon, O. Zilberberg, and I. Carusotto, "Topological Photonics," ArXiv e-prints (2018), arXiv:1802.04173 [physics.optics].
[42] Ling Lu, John D. Joannopoulos, and Marin Soljacic, "Topological photonics," Nat Photon **8**, 821–829 (2014).
[43] Ramy El-Ganainy, Konstantinos G Makris, Mercedeh Khajavikhan, Ziad H Musslimani, Stefan Rotter, and Demetrios N Christodoulides, "Non-hermitian physics and pt symmetry," Nature Physics **14**, 11 (2018).
[44] S. Longhi, "Parity-Time Symmetry meets Photonics: A New Twist in non-Hermitian Optics," ArXiv e-prints (2018), arXiv:1802.05025 [physics.optics].
[45] V. Kozii and L. Fu, "Non-Hermitian Topological Theory of Finite-Lifetime Quasiparticles: Prediction of Bulk Fermi Arc Due to Exceptional Point," ArXiv e-prints (2017), arXiv:1708.05841 [cond-mat.mes-hall].
[46] M. Papaj, H. Isobe, and L. Fu, "Bulk Fermi arc of disordered Dirac fermions in two dimensions," ArXiv e-prints (2018), arXiv:1802.00443 [cond-mat.dis-nn].
[47] H. Shen and L. Fu, "Quantum Oscillation from In-gap States and non-Hermitian Landau Level Problem," ArXiv e-prints (2018), arXiv:1802.03023 [cond-mat.str-el].
[48] Kenta Esaki, Masatoshi Sato, Kazuki Hasebe, and Mahito Kohmoto, "Edge states and topological phases in non-hermitian systems," Phys. Rev. B **84**, 205128 (2011).
[49] Tony E. Lee, "Anomalous edge state in a non-hermitian lattice," Phys. Rev. Lett. **116**, 133903 (2016).
[50] Daniel Leykam, Konstantin Y. Bliokh, Chunli Huang, Y. D. Chong, and Franco Nori, "Edge modes, degeneracies, and topological numbers in non-hermitian systems," Phys. Rev. Lett. **118**, 040401 (2017).
[51] Henri Menke and Moritz M. Hirschmann, "Topological quantum wires with balanced gain and loss," Phys. Rev. B **95**, 174506 (2017).
[52] Simon Lieu, "Topological phases in the non-hermitian su-schrieffer-heeger model," Phys. Rev. B **97**, 045106 (2018).
[53] Huitao Shen, Bo Zhen, and Liang Fu, "Topological band theory for non-hermitian hamiltonians," Phys. Rev. Lett. **120**, 146402 (2018).
[54] Chuanhao Yin, Hui Jiang, Linhu Li, Rong Lü, and Shu Chen, "Geometrical meaning of winding number and its characterization of topological phases in one-dimensional chiral non-hermitian systems," Phys. Rev. A **97**, 052115 (2018).
[55] C. Li, X. Z. Zhang, G. Zhang, and Z. Song, "Topological phases in a kitaev chain with imbalanced pairing," Phys. Rev. B **97**, 115436 (2018).
[56] M. S. Rudner and L. S. Levitov, "Topological transition in a non-hermitian quantum walk," Phys. Rev. Lett. **102**, 065703 (2009).
[57] Shi-Dong Liang and Guang-Yao Huang, "Topological invariance and global berry phase in non-hermitian systems," Phys. Rev. A **87**, 012118 (2013).
[58] Yi Chen Hu and Taylor L. Hughes, "Absence of topological insulator phases in non-hermitian *pt*-symmetric hamiltonians," Phys. Rev. B **84**, 153101 (2011).
[59] Zongping Gong, Sho Higashikawa, and Masahito Ueda, "Zeno hall effect," Phys. Rev. Lett. **118**, 200401 (2017).
[60] Jiangbin Gong and Qing-hai Wang, "Geometric phase in $\mathcal{PT}$-symmetric quantum mechanics," Phys. Rev. A **82**, 012103 (2010).
[61] M. S. Rudner, M. Levin, and L. S. Levitov, "Survival, decay, and topological protection in non-Hermitian quantum transport," ArXiv e-prints (2016), arXiv:1605.07652 [cond-mat.mes-hall].
[62] Kohei Kawabata, Yuto Ashida, Hosho Katsura, and Masahito Ueda, "Parity-time-symmetric topological superconductor," arXiv preprint arXiv:1801.00499 (2018).
[63] X. Ni, D. Smirnova, A. Poddubny, D. Leykam, Y. Chong, and A. B. Khanikaev, "Exceptional points in topological edge spectrum of PT symmetric domain walls," ArXiv e-prints (2018), arXiv:1801.04689 [cond-mat.mes-hall].
[64] A. A. Zyuzin and A. Yu. Zyuzin, "Flat band in disorder-driven non-hermitian weyl semimetals," Phys. Rev. B **97**, 041203 (2018).
[65] Alexander Cerjan, Meng Xiao, Luqi Yuan, and Shanhui Fan, "Effects of non-hermitian perturbations on weyl hamiltonians with arbitrary topological charges," Phys. Rev. B **97**, 075128 (2018).
[66] L. Zhou, Q.-h. Wang, H. Wang, and J. Gong, "Dynamical quantum phase transitions in non-Hermitian lattices," ArXiv e-prints (2017), arXiv:1711.10741 [cond-mat.stat-mech].
[67] J. González and R. A. Molina, "Topological protection from exceptional points in weyl and nodal-line semimetals," Phys. Rev. B **96**, 045437 (2017).
[68] Marcel Klett, Holger Cartarius, Dennis Dast, Jörg Main, and Günter Wunner, "Relation between $\mathcal{PT}$-symmetry breaking and topologically nontrivial phases in the su-schrieffer-heeger and kitaev models," Phys. Rev. A **95**, 053626 (2017).
[69] M. Klett, H. Cartarius, D. Dast, J. Main, and G. Wunner, "Topological edge states in the Su-Schrieffer-Heeger model subject to balanced particle gain and loss," ArXiv e-prints (2018), arXiv:1802.06128 [quant-ph].
[70] C. Yuce, "Majorana edge modes with gain and loss," Phys. Rev. A **93**, 062130 (2016).
[71] Cem Yuce, "Topological phase in a non-hermitian pt symmetric system," Physics Letters A **379**, 1213–1218 (2015).
[72] Yong Xu, Sheng-Tao Wang, and L.-M. Duan, "Weyl exceptional rings in a three-dimensional dissipative cold atomic gas," Phys. Rev. Lett. **118**, 045701 (2017).
[73] Wenchao Hu, Hailong Wang, Perry Ping Shum, and Y. D. Chong, "Exceptional points in a non-hermitian topological pump," Phys. Rev. B **95**, 184306 (2017).
[74] Xiaohui Wang, Tingting Liu, Ye Xiong, and Peiqing Tong, "Spontaneous $\mathcal{PT}$-symmetry breaking in non-hermitian kitaev and extended kitaev models," Phys. Rev. A **92**, 012116 (2015).
[75] Shaolin Ke, Bing Wang, Hua Long, Kai Wang, and Peixiang Lu, "Topological edge modes in non-hermitian plasmonic waveguide arrays," Optics Express **25**, 11132–11143 (2017).
[76] Nicolas X. A. Rivolta, Henri Benisty, and Bjorn Maes, "Topological edge modes with $\mathcal{PT}$ symmetry in a quasiperiodic structure," Phys. Rev. A **96**, 023864 (2017).

[77] Z. Gong, Y. Ashida, K. Kawabata, K. Takasan, S. Higashikawa, and M. Ueda, "Topological phases of non-Hermitian systems," ArXiv e-prints (2018), arXiv:1802.07964v1 [cond-mat.mes-hall].

[78] Gal Harari, Miguel A Bandres, Yaakov Lumer, Mikael C Rechtsman, YD Chong, Mercedeh Khajavikhan, Demetrios N Christodoulides, and Mordechai Segev, "Topological insulator laser: Theory," Science , eaar4003 (2018).

[79] Julia M. Zeuner, Mikael C. Rechtsman, Yonatan Plotnik, Yaakov Lumer, Stefan Nolte, Mark S. Rudner, Mordechai Segev, and Alexander Szameit, "Observation of a topological transition in the bulk of a non-hermitian system," Phys. Rev. Lett. **115**, 040402 (2015).

[80] Xiang Zhan, Lei Xiao, Zhihao Bian, Kunkun Wang, Xingze Qiu, Barry C. Sanders, Wei Yi, and Peng Xue, "Detecting topological invariants in nonunitary discrete-time quantum walks," Phys. Rev. Lett. **119**, 130501 (2017).

[81] L. Xiao, X. Zhan, Z. H. Bian, K. K. Wang, X. Zhang, X. P. Wang, J. Li, K. Mochizuki, D. Kim, N. Kawakami, W. Yi, H. Obuse, B. C. Sanders, and P. Xue, "Observation of topological edge states in parity–time-symmetric quantum walks," Nature Physics **13**, 1117 (2017).

[82] S Weimann, M Kremer, Y Plotnik, Y Lumer, S Nolte, KG Makris, M Segev, MC Rechtsman, and A Szameit, "Topologically protected bound states in photonic parity–time-symmetric crystals," Nature materials **16**, 433 (2017).

[83] M. Parto, S. Wittek, H. Hodaei, G. Harari, M. A. Bandres, J. Ren, M. C. Rechtsman, M. Segev, D. N. Christodoulides, and M. Khajavikhan, "Complex Edge-State Phase Transitions in 1D Topological Laser Arrays," ArXiv e-prints (2017), arXiv:1709.00523 [physics.optics].

[84] H. Zhao, P. Miao, M. H. Teimourpour, S. Malzard, R. El-Ganainy, H. Schomerus, and L. Feng, "Topological Hybrid Silicon Microlasers," ArXiv e-prints (2017), arXiv:1709.02747 [physics.optics].

[85] H. Zhou, C. Peng, Y. Yoon, C. W. Hsu, K. A. Nelson, L. Fu, J. D. Joannopoulos, M. Soljacic, and B. Zhen, "Observation of Bulk Fermi Arc and Polarization Half Charge from Paired Exceptional Points," ArXiv e-prints (2017), arXiv:1709.03044 [physics.optics].

[86] Y. Xiong, "Why does bulk boundary correspondence fail in some non-hermitian topological models," ArXiv e-prints (2017), arXiv:1705.06039v1 [cond-mat.mes-hall].

[87] Stefano Longhi, "Nonadiabatic robust excitation transfer assisted by an imaginary gauge field," Phys. Rev. A **95**, 062122 (2017).

[88] Naomichi Hatano and David R. Nelson, "Localization transitions in non-hermitian quantum mechanics," Phys. Rev. Lett. **77**, 570–573 (1996).

[89] W_P Su, JR Schrieffer, and AJ Heeger, "Soliton excitations in polyacetylene," Physical Review B **22**, 2099 (1980).

[90] Related models have been studied, for example, in Refs. [52, 54, 97].

[91] Charles Poli, Matthieu Bellec, Ulrich Kuhl, Fabrice Mortessagne, and Henning Schomerus, "Selective enhancement of topologically induced interface states in a dielectric resonator chain," Nature communications **6**, 6710 (2015).

[92] We note that the numerical precision of Ref.[49] is improvable. According to our exact results, the zero-mode line in their Fig. 3(a) should span the entire $[-1/\sqrt{2}, 1/\sqrt{2}]$ interval, instead of the two disconnected lines there.

[93] Supplemental Material.

[94] Recently we noticed Ref.[98], in which similar localization is found numerically; however, in contrast to our viewpoint, it is suggested there that the localization lessens the relevance of zero modes and destroys bulk-boundary correspondence. Also note that the zero-mode interval in their Fig.1 differs from our exact solutions.

[95] We emphasize that the bulk energy spectra remain insensitive to a small perturbation at the ends of a long chain. In fact, the eigenstates of $H^\dagger$ (namely left eigenstates) have opposite exponential decay and the outcome of a perturbation depends on the product of right and left eigenstates.

[96] For example, we find that it is the case for the model numerically studied in Ref. [52].

[97] Baogang Zhu, Rong Lü, and Shu Chen, "$\mathcal{PT}$ symmetry in the non-hermitian su-schrieffer-heeger model with complex boundary potentials," Phys. Rev. A **89**, 062102 (2014).

[98] V. M. Martinez Alvarez, J. E. Barrios Vargas, and L. E. F. Foa Torres, "Non-hermitian robust edge states in one dimension: Anomalous localization and eigenspace condensation at exceptional points," Phys. Rev. B **97**, 121401 (2018).

Supplemental Material

Two supplemental figures.–As explained in the main article, the equation $|\beta_1(E)| = |\beta_2(E)|$ determines the bulk-band energies [see the discussion below Eq. (12) in the main article]. In fact, in the complex E plane, $|\beta_1(E)| = |\beta_2(E)|$ determines one-dimensional curves containing the bulk-band energies. Fig.6 illustrates calculating bulk-band energies by solving $|\beta_1(E)| = |\beta_2(E)|$ for three values of t_1.

Fig.7 shows the energies and topological invariant for the parameter regime $|t_2| < |\gamma/2|$ (In the main article, we have focused on $|t_2| > |\gamma/2|$).

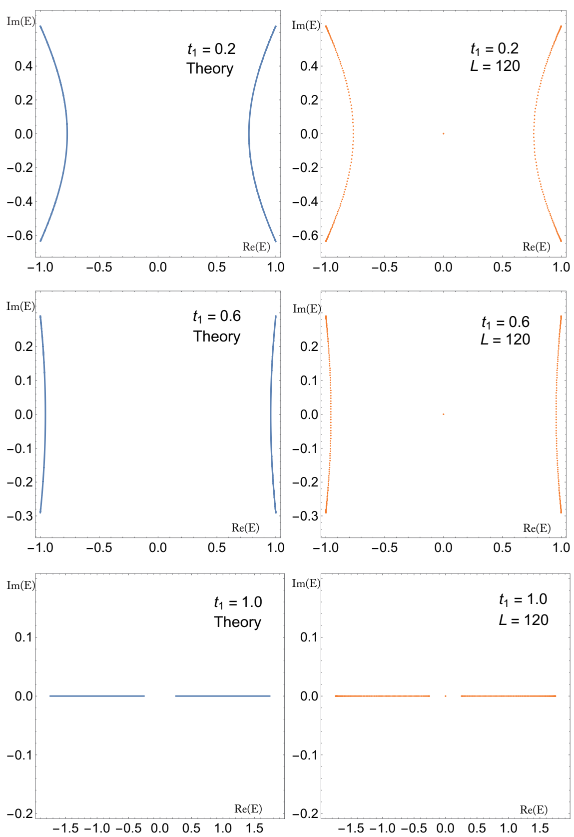

FIG. 6. Left panels: Energies (E) solved from $|\beta_1(E)| = |\beta_2(E)|$ [see the discussion below Eq.(12) in the main article]; Right panels: Numerical eigenenergies of open chains with length $L = 120$. Common parameters are $t_2 = 1, \gamma = 4/3$.

Nonzero t_3.–Let us outline the calculation of generalized Brillouin zone C_β for nonzero t_3. We consider an open-boundary chain with length L. In the bulk, the real-space eigenequations are $t_2\psi_{n-1,B} + (t_1 + \frac{\gamma}{2})\psi_{n,B} + t_3\psi_{n+1,B} = E\psi_{n,A}$ and $t_3\psi_{n-1,A} + (t_1 - \frac{\gamma}{2})\psi_{n,A} + t_2\psi_{n+1,A} = E\psi_{n,B}$. Similar to Eq.

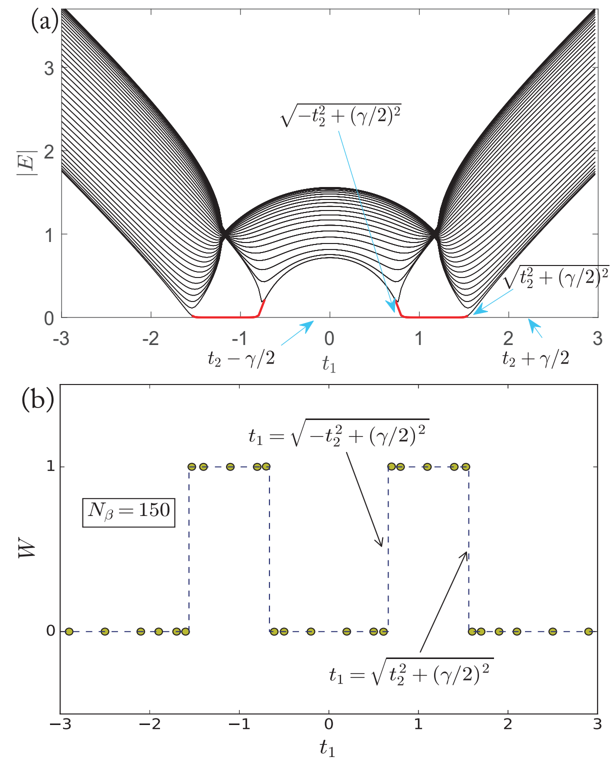

FIG. 7. (a) The modulus of energy for an open chain with length $L = 40$. (b) Numerical results of the topological invariant. $t_2 = 1.0, \gamma = 2.4$. According to the analytical solution, in the regime $|t_2| < |\gamma|/2$, there are four transition points $t_1 = \pm\sqrt{\pm t_2^2 + (\gamma/2)^2}$. The theory is consistent with the numerical results. The topological invariant correctly predicts the number of zero modes.

(6) of the main article, we now have

$$\begin{aligned}
[t_2\beta^{-1} + (t_1 + \frac{\gamma}{2}) + t_3\beta]\phi_B &= E\phi_A, \\
[t_3\beta^{-1} + (t_1 - \frac{\gamma}{2}) + t_2\beta]\phi_A &= E\phi_B.
\end{aligned} \tag{21}$$

Therefore, β and E satisfy

$$E^2 = [t_2\beta^{-1} + (t_1 + \gamma/2) + t_3\beta][t_3\beta^{-1} + (t_1 - \gamma/2) + t_2\beta]. \tag{22}$$

As a quartic equation of β, it has four roots $\beta_j(E)$ ($j = 1, 2, 3, 4$). As explained in the main article, the bulk-band energies have to satisfy $|\beta_i(E)| = |\beta_j(E)|$ for a pair of i, j. In fact, this equation can also be intuitively understood as follows. Suppose that a wave with β_i propagates from the left end towards the right. It hits the right end and gets reflected, and the reflected waves with β_j propagates back to the left end. To satisfy certain standing-wave conditions for an energy eigenstate, the magnitudes of the initial and the final waves have to be of the same order, therefore, one must have $|\beta_i(E)|^L \sim |\beta_j(E)|^L$ or $|\beta_i(E)| = |\beta_j(E)|$. Each equation $|\beta_i(E)| = |\beta_j(E)|$ determines a one-dimensional curve in the complex E plane, and the β curve follows from the E curves.

There is also a more brute-force approach to find the C_β curve. One can numerically solve the eigen-energies of an open chain, and then find $\beta_j(E)$'s from Eq. (22). In this calculations, one has to discard $\beta_i(E), \beta_j(E)$ that do not satisfy $|\beta_i(E)| = |\beta_j(E)|$, as they should not be regarded as bulk components of the eigenstates. This disposal is similar to the Hermitian case: A typical eigenstate of an open chain is a superposition of right-propagating and left-propagating Bloch waves (both have $|\beta| = 1$) and certain decaying components localized at the two ends. The (Hermitian) topological invariants are defined in terms of the bulk components, namely the Bloch waves.